Pre-Steady-State Kinetic Analysis of 2-Hydroxy-6-keto-nona-2,4-diene-1,9-dioic Acid 5,6-Hydrolase: Kinetic Evidence for Enol/Keto Tautomerization†

Ian M. J. Henderson and Timothy D. H. Bugg*

Department of Chemistry, University of Southampton, Highfield, Southampton SO17 1BJ, U.K.

Received May 13, 1997; Revised Manuscript Received July 17, 1997⊗

ABSTRACT: The reaction catalyzed by 2-hydroxy-6-keto-nona-2,4-diene-1,9-dioic acid 5,6-hydrolase (MhpC) was analyzed by stopped-flow UV−visible kinetics at 317 nm (substrate depletion) and 270 nm (product formation) at pH 5.0 and 4.0. Comparison of the rates and amplitudes of product formation versus substrate depletion provided evidence for the formation of a discrete keto-intermediate, as predicted from previous isotope exchange experiments [Lam, W. W. Y., & Bugg, T. D. H. (1997) *Biochemistry, 36*, 12242−12251]. Accurate modeling of the concentration data could only be achieved using a branched kinetic mechanism in which the intermediate is released at a rate comparable to its catalytic turnover, consistent with the earlier isotope exchange data. The apparent "leakiness" of the active site and relatively weak substrate binding (K_d = 30 μM) are consistent with a mechanism in which the enzyme binds the dienol substrate in a strained, nonplanar conformation which promotes ketonization in the C-5 position to give a keto-intermediate.

Enzyme-catalyzed hydrolytic cleavage of carbon−carbon bonds is an unusual process and requires the presence of a suitable electron sink to assist C−C bond cleavage. Two examples are the β-diketone hydrolase from beef liver, which utilizes a β-diketone as an electron sink (Hsiang et al., 1972), and kynureninase from *Pseudomonas fluorescens*, which utilizes pyridoxal 5′-phosphate to create a β-iminium linkage during its catalytic cycle (Phillips & Dua, 1991).

The hydrolytic cleavage of dienol ring fission products on bacterial *meta*-cleavage pathways is catalyzed by a family of C−C hydrolase enzymes. We have purified and characterized 2-hydroxy-6-keto-nona-2,4-diene-1,9-dioic acid 5,6-hydrolase from *Escherichia coli*, and we have demonstrated that the enzyme-catalyzed reaction proceeds with retention of stereochemistry at C-5 (Lam & Bugg, 1997). On the basis of chemical precedent, we have proposed a mechanistic scheme shown in Scheme 2 involving tautomerization of the substrate dienol (RFP)[1] to give a keto-intermediate (RFP^k). This intermediate contains an α,β-unsaturated ketone which can function as an electron sink for a stereospecific C−C fragmentation reaction, to give the products 2-hydroxypentadienoic acid (HPD) and succinic acid.

Several other enzymes have been found to catalyze the interconversion of keto and enol tautomers. In cases such as ketosteroid isomerase (Kuliopulos et al., 1991) and oxalocrotonate tautomerase (Whitman et al., 1991, 1992), the substrate is the keto tautomer, which is isomerized to give an enolic intermediate. In contrast the substrate for hydrolase, MhpC has been shown to exist as a stable dienol, which is thought to be converted to a keto tautomer during the reaction (Lam & Bugg, 1994). It is therefore of interest to determine the type of catalytic processes involved in such a tautomerization process.

Scheme 1: Generalized Reaction Scheme for C−C Hydrolases

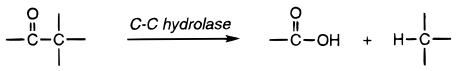

Scheme 2: Proposed Mechanistic Scheme for the MhpC-Catalyzed Reaction, Illustrating the Keto-Intermediate (RFP^k)[a]

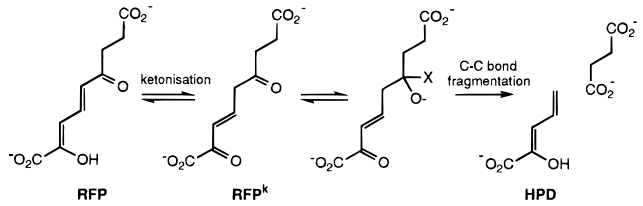

[a] X is either OH (from attack of water) or an active site nucleophile.

Evidence from ^2H isotope exchange presented in the previous paper in this issue is consistent with a keto-intermediate (RFP^k) which is formed rapidly in the catalytic cycle but which is partially released by the enzyme (Lam & Bugg, 1997). In order to characterize further the catalytic cycle of hydrolase MhpC, we have undertaken an analysis of the enzymatic reaction using stopped-flow reaction kinetics. The results reported herein provide further evidence for the keto-intermediate and offer a rationalization of the catalytic processes involved in C−C hydrolases.

MATERIALS AND METHODS.

Materials. 2,3-Dihydroxyphenylpropionic acid was prepared by the method of Blakley and Simpson (1963). Other chemicals and biochemicals were purchased from Aldrich or Sigma Chemical Co.

† This work is supported by BBSRC (Grant B04835) and the Royal Society.

* Author to whom correspondence should be addressed. Tel: 01703-593816. Fax: 01703-593781. Email: tdb@soton.ac.uk.

⊗ Abstract published in *Advance ACS Abstracts,* September 15, 1997.

[1] Abbreviations: DHP, 2,3-dihydroxyphenylpropionic acid; HPD, 2-hydroxypentadienoic acid; RFP, ring fission product (2-hydroxy-6-keto-nona-2,4-diene-1,9-dioic acid); RFP^k, ketonized ring fission product (2,6-diketo-non-3-ene 1,9-dioic acid); MhpB, 2,3-dihydroxyphenylpropionate 1,2-dioxygenase; MhpC, 2-hydroxy-6-keto-nona-2,4-diene-1,9-dioic acid 5,6-hydrolase.

S0006-2960(97)01116-1 CCC: $14.00

Purification and Preparation of MhpC. *E. coli* MhpC was purified from the overexpression strain *E. coli* W3110/pTB9 as described elsewhere (Lam & Bugg, 1997), except that the purification buffer used throughout was 50 mM potassium phosphate (pH 7.0) containing 10 mM 2-mercaptoethanol. Following phenyl agarose hydrophobic interaction chromatography and Q sepharose anion exchange chromatography, the pooled fractions were dialyzed against 2 l of 50 mM potassium phosphate (pH 7.0). The resultant pool had a specific activity of 32.1 units mg^{-1} at a protein concentration of 0.2 mg mL^{-1}. SDS−PAGE showed this preparation to be >90% pure, and assays showed it to be free of MhpB and MhpD enzyme activities.

For stopped-flow experiments, 15 mL of MhpC was dialyzed against 10 mM buffer of the desired pH. The volume was measured and freeze-dried. The resulting solid was dissolved in $^1/_5$ measured volume after dialysis of distilled water. Assay showed that 75% activity was retained, resulting in a 3.75-fold increase in concentration to 24 units mL^{-1}, equal to 9.65 μM active site concentration.

RFP Preparation and MhpC Assay. 2-Hydroxy-6-oxonona-2,4-diene-1,9-dioic acid (ring fission product, RFP) was prepared enzymatically from 2,3-dihydroxyphenylpropionate (DHP) using 2,3-dihydroxy-phenylpropionate 1,2-dioxygenase (MhpB). The MhpB enzyme activity was obtained as a byproduct from the phenyl agarose column during the purification of MhpC. The procedure was as previously described (Lam & Bugg, 1997), except that 400 units (2 mL) of MhpB holoenzyme was used to convert 100 mg of DHP, by gradual addition of 200 μL aliquots.

MhpC was assayed routinely in 50 mM potassium phosphate (pH 8.0) with 50 μM RFP. The decrease in absorbance at 394 nm was recorded and activity calculated using $\epsilon = 15\ 600\ M^{-1}\ cm^{-1}$. Measurements of K_M and k_{cat} at pH 4.0 and 5.0 were carried out in 50 mM sodium citrate buffer at the appropriate pH. The reaction was monitored at 317 nm using ϵ values of 16 200 and 15 000 $M^{-1}\ cm^{-1}$ for pH 4.0 and 5.0, respectively.

Stopped-Flow Experiments. Stopped-flow experiments were carried out using a Hi-Tech SFA-20 rapid kinetics accessory attached to a Cary-1 UV−visible spectrophotometer. Enzyme concentrations were determined by assay at pH 8.0. Substrate concentrations were measured in a standard cuvette at the pH of the experiment using the known ϵ value. Disappearance of substrate was monitored at 317 nm, and appearance of product was monitored at 270 nm.

Single shots were stored as single data files within the Cary operating system. These were converted to ASCII files and exported to an external graph drawing program. Data files from single shots (at least three) were then averaged. Data were then fitted to either a double exponential decay (substrate) or eq 1 (product) to determine the total change in absorbance allowing for a dead time of 33 ms.

$$y = A(1 - e^{-kt}) \quad (1)$$

Knowledge of the total change in absorbance and the initial RFP concentration enabled the conversion of the data to concentration vs time. Simulations were carried out using a fourth-order Runge−Kutta algorithm (Press et al., 1986) written in Visual BASIC and running on a 486-DX2 PC. A time step of 0.5 ms was used. The initial binding of substrate to the enzyme was assumed to be very fast, and was therefore treated by the quasi-equilibrium method of Cha (1969). For example, using Scheme 1, at the beginning of each iteration, the concentration of E·RFP was calculated from E_o, RFP_o, and K_s using the quadratic binding equation (eq 2).

$$[E\cdot RFP] = \frac{(E_o + RFP_o + K_s) - \sqrt{(E_o + RFP_o + K_s)^2 - 4E_oRFP_o}}{2} \quad (2)$$

This was subtracted from E_o and RFP_o to give the temporary values E_{tmp} and RFP_{tmp}. The Runge−Kutta procedure was carried out on all the other species present in the mechanism, including ES to give new values. The values of E_o and RFP_o for the next iteration were calculated according to eq 3.

$$E_o = E_{tmp} + E\cdot RFP_{new} + \Delta\text{succinate}$$
$$RFP_o = RFP_{tmp} + E\cdot RFP_{new} \quad (3)$$

RESULTS

The pH/rate profile determined previously for MhpC shows a typical bell-shaped curve with pK_a values of 6.5 and 9.0 (Lam & Bugg, 1997). It was decided to study the pre-steady-state kinetic behavior of MhpC at acidic pH in order to slow the reaction down sufficiently to allow it to be observed and also to stabilize any putative acyl enzyme intermediates, which for the serine proteases are known to be highly stabilized under acidic pH (Balls & Wood, 1956). First of all the steady-state kinetic behavior of MhpC at the desired pH was analyzed. Initial rate vs [RFP] plots at pH 4.0 and 5.0 show classical Michaelis−Menten kinetics, and the deduced kinetic constants are given in Table 1. At pH 5.0, the turnover number is 3.9 s^{-1}, reduced 9-fold from the value of 36 s^{-1} at pH 8.0, and at pH 4.0 k_{cat} is further reduced at 1.0 s^{-1}.

Table 1: Steady-State Kinetic Parameters for MhpC Measured at pH 4.0 and 5.0 in 50 mM Citrate Buffer[a]

pH	K_M (μM)	k_{cat} (s^{-1})
5.0	4.1 ± 0.6	3.9 ± 0.2
4.0	7.0 ± 0.5	1.0 ± 0.2

[a] Values were determined by nonlinear regression fitting to the Michaelis−Menten equation. Values of k_{cat} are based on a subunit molecular mass of 29 000 Da for MhpC.

A single stopped-flow experiment was carried out at pH 5.0. The absorbance traces for substrate and product were analyzed as described in Materials and Methods, allowing for a dead time of 33 ms. Knowledge of the total absorbance change during the stopped-flow experiment and of the initial substrate concentration determined by measurement of the absorbance of a sample in a standard cuvette allows the conversion of the stopped-flow absorbance traces to plots of concentration versus time (see Figure 1).

The kinetic parameters which gave the best fit to the experimental data are given in Table 2. The disappearance of substrate at 317 nm can be described by a double-exponential decay with rate constants of 10.3 and 2.6 s^{-1}. The appearance of product at 270 nm is described by a single exponential with a rate constant of 3.0 s^{-1}. These rate constants are indicative of a two-step kinetic mechanism in

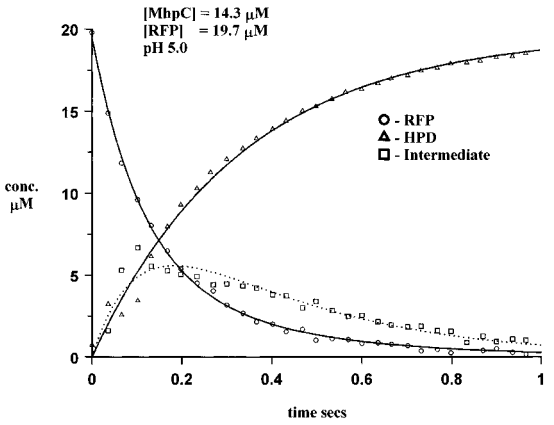

FIGURE 1: Pre-steady-state kinetic data measured for the MhpC-catalyzed reaction in 50 mM sodium citrate buffer, pH 5.0. Substrate consumption measured at 317 nm, product appearance measured at 270 nm, intermediate concentration data inferred by subtraction from starting substrate concentration. Substrate consumption and intermediate data fitted to double exponentials, product data fitted to single exponential (see Table 2 for rate constants).

Table 2: Descriptive Parameters of a Stopped-Flow Experiment at pH 5.0[a]

λ (nm)	k_1 (s^{-1})	k_2 (s^{-1})	$A_1 \times 10^3$	$A_2 \times 10^3$
317	10.3 ± 0.5	2.6 ± 0.1	141 ± 5	64 ± 4
270	3.02 ± 0.05		354 ± 1	

[a] The concentrations of RFP and MhpC were 19.7 and 14.3 μM, respectively. Disappearance of RFP (317 nm) was described by a double-exponential decay. Appearance of HPD (270 nm) was described by eq 1.

which substrate is converted rapidly (10 s^{-1}) to an intermediate, which is converted to product more slowly (3 s^{-1}).

If no intermediates accumulate during a reaction, the sum of the substrate and product should always equal the initial substrate concentration. This is not the case in this instance, and Figure 1 shows the plot of concentration vs time for the substrate, product, and putative intermediate (as the sum of the substrate and product subtracted from the initial substrate concentration). The concentration data for the inferred intermediate can also be described by a double exponential: the intermediate accumulates with a rate constant of 10 s^{-1} and decays with a rate constant of 3 s^{-1}. These data are entirely consistent with the existence of a kinetically competent intermediate formed in the MhpC reaction cycle.

In an attempt to gain further information concerning this intermediate, experiments were carried out at pH 4.0, where the reaction is even slower than at pH 5.0, and conditions ranging from single turnover to >3 turnovers. The absorbance traces are shown in Figure 2. Once again the disappearance of substrate at 317 nm could be described by a double exponential and the appearance of product at 270 nm by a single exponential, as shown in Figure 2. The determined rate constants and amplitudes are given in Table 3. As found for the pH 5.0 dataset, substrate disappearance was characterized by a fast step ($k_1 = 13-25$ s^{-1}), followed by a slow step ($k_2 = 0.6-1.5$ s^{-1}), the latter step matching the rate constant for product formation ($k = 0.6-1.3$ s^{-1}), consistent with a rapidly formed intermediate.

The first rate constant for substrate disappearance increases with increasing substrate concentration, which can be rationalized by higher concentrations of the ES complex at higher substrate concentrations, therefore implying that the

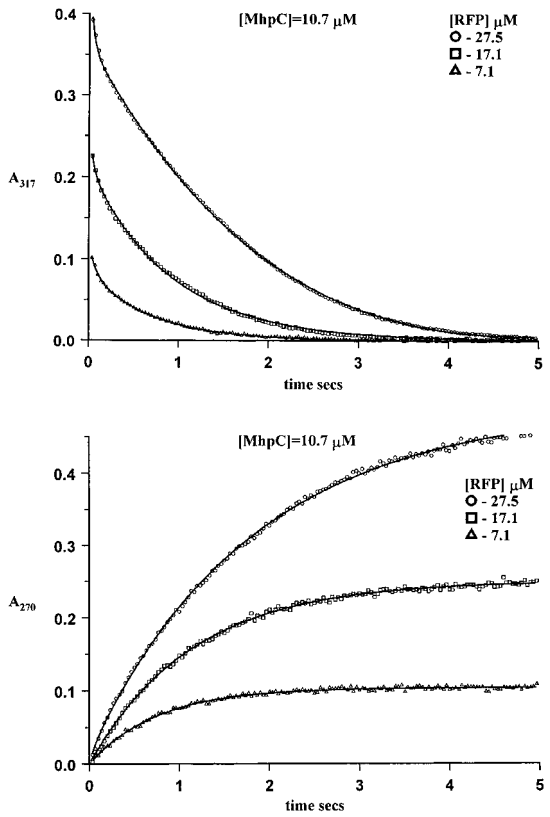

FIGURE 2: Pre-steady-state kinetic data measured for the MhpC-catalyzed reaction in 50 mM sodium citrate buffer, pH 4.0. Substrate consumption measured at 317 nm, product appearance measured at 270 nm. Substrate consumption and intermediate data fitted to double exponentials, product data fitted to single exponential (see Table 3 for rate constants).

Table 3: Descriptive Parameters of a Stopped-Flow Experiment at pH 4.0[a]

(a) 317 nm

[RFP] (μM)	k_1 (s^{-1})	k_2 (s^{-1})	$A_1 \times 10^3$	$A_2 \times 10^3$
7.1	13 ± 1	1.5 ± 0.02	36 ± 0.2	84 ± 0.9
17.1	23 ± 4	1.1 ± 0.01	51 ± 0.8	211 ± 0.9
32.7	25 ± 6	0.6 ± 0.1	380 ± 5	40 ± 0.4

(b) 270 nm

[RFP] (μM)	k_1 (s^{-1})	$A_1 \times 10^3$
7.1	1.33 ± 0.02	104 ± 0.3
17.1	0.88 ± 0.01	249 ± 0.5
32.7	0.57 ± 0.002	482 ± 0.3

[a] The concentration of MhpC was 9.65 μM. Disappearance of RFP (a) was described by a double-exponential decay. Appearance of HPD (b) was described by eq 1.

enzyme is saturated with substrate only at substrate concentrations of >20 μM. The second rate constant and the rate constant for product appearance decrease with increasing substrate concentration. This can be explained if the HPD (the observed product) is released before the slowest step on the complete pathway. Thus, at [RFP] = 7.1 μM, under single-turnover conditions (where [S] < [E]), the slowest step has no influence on the observed rates. However, in multiple-turnover experiments (where [S] > [E]), the slowest step becomes important as it determines the rate at which free enzyme becomes available. There is no significant burst of HPD production evident, indicating that the final step (release of succinate) is not greatly slower than the preceding steps.

Scheme 3: Kinetic Mechanisms Used to Simulate the MhpC Pre-Steady-State Kinetic Data[a]

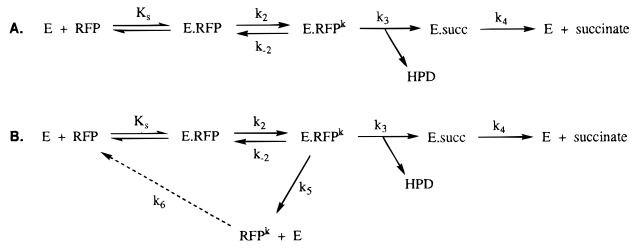

[a] (A) Linear kinetic model; (B) Branched kinetic model, involving release of intermediate RFP^k.

Table 4: Rate Constants Used in the Simulation of Stopped-Flow Experiments at pH 4.0 Using the Linear Kinetic Model[a]

step	symbol	value
$E + RFP \leftrightarrow E{\cdot}RFP$	K_S	1000 μM
$E{\cdot}RFP \rightarrow E{\cdot}RFP^k$	k_2	200 s^{-1}
$E{\cdot}RFP^k \leftarrow E{\cdot}RFP$	k_{-2}	2 s^{-1}
$E{\cdot}RFP^k \rightarrow E{\cdot}succ + HPD$	k_3	11 s^{-1}
$E{\cdot}succ \rightarrow E + succinate$	k_4	1.8 s^{-1}

[a] Concentrations of RFP and MhpC were as in Table 3.

Simulations of the pH 4.0 datasets were carried out using a linear four-step kinetic model, as shown in Scheme 3A. It was found that the values given in Table 4 were the only ones that could describe all the pH 4.0 datasets simultaneously. The striking feature of these kinetic data is the very high K_s value (1 mM) for substrate binding, which is followed by a rapid (200 s^{-1}) and almost irreversible conversion to $E{\cdot}RFP^k$. The predicted fits for the concentration vs time datasets are shown in Figure 3. Good correlation is observed for both substrate disappearance and product appearance, although slight deviation is observed for the initial time points (<100 ms) in the substrate disappearance data. K_M and k_{cat} values can be calculated for the kinetic mechanism in Scheme 3A, as shown by eq 4.

$$k_{cat} = \frac{k_2 k_3 k_4}{k_4(k_2 + k_{-2} + k_3) + k_2 k_3}$$

$$K_M = \frac{K_S k_4(k_{-2} + k_3)}{k_4(k_2 + k_{-2} + k_3) + k_2 k_3} \qquad (4)$$

The calculated values of k_{cat} and K_M of 1.5 s^{-1} and 9.1 μM are in good agreement with the experimental values of 1.0 s^{-1} and 7.0 μM. However, the predicted concentration profile for the intermediate $E{\cdot}RFP^k$, as shown in Figure 4, does not fit at all well with the observed data points. The apparent rate constants for the formation (k_2 = 200 s^{-1}) and decay (k_3 = 11 s^{-1}) of the intermediate $E{\cdot}RFP^k$ predict a much sharper decay in the concentration of the intermediate than is observed by experiment. This suggests that some of the intermediate escapes into solution, where it decays slowly, either to substrate or to product.

In view of the surprisingly high value for K_S and the relatively poor fit for the intermediate concentration data, the kinetic mechanism was modified to allow for release of the keto-intermediate RFP^k and its subsequent recycling via nonenzymatic enolization to RFP. This branched kinetic model is shown in Scheme 3B. Release of the intermediate RFP^k from the MhpC active site was predicted from the ^2H

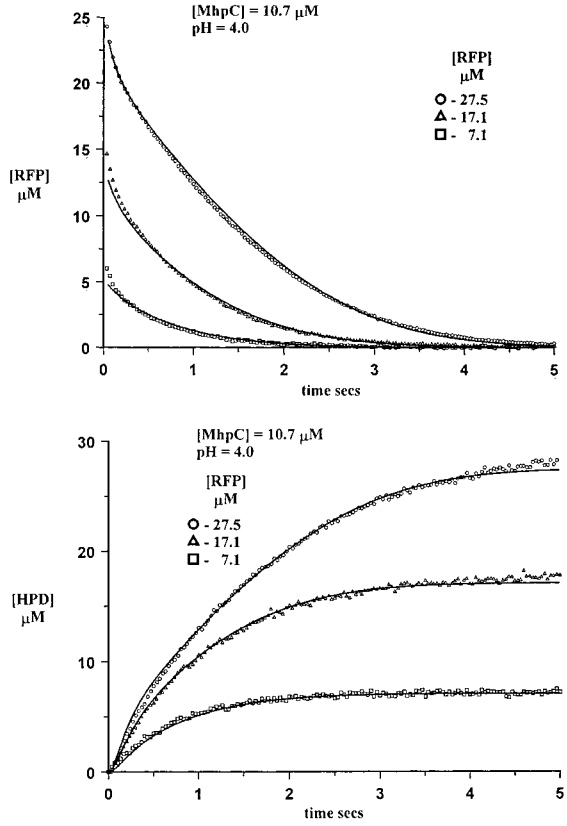

FIGURE 3: Pre-steady-state kinetic data measured for the MhpC-catalyzed reaction in 50 mM sodium citrate buffer, pH 4.0, modeled by linear kinetic model (see Scheme 3A).

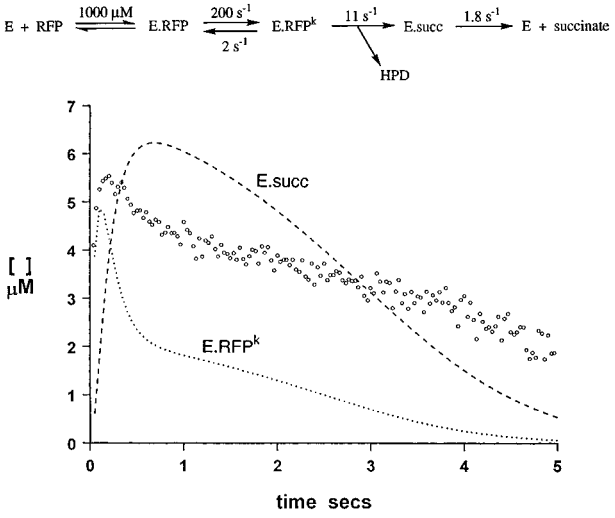

FIGURE 4: Intermediate ($E{\cdot}RFP^k$) concentrations observed and calculated from the linear kinetic model for the [RFP] = 27.5 μM dataset. Inferred intermediate concentration (circles) calculated by substraction of [RFP] and [HPD] from initial substrate concentration. Calculated values of [$E{\cdot}RFP^k$] (dotted line) and [$E{\cdot}succ$] (dashed line) are shown.

exchange results presented in the previous paper is this issue, and would intuitively give rise to higher levels of intermediate in solution. It is assumed in this model that the release of RFP^k from the enzyme active site is irreversible. If the enzyme were able to bind RFP^k from solution, then in the presence of ^2H_2O the enzyme would bind stereorandom ^2H-RFP^k, and hence would not be entirely stereospecific in the H-5_E position (Lam & Bugg, 1997). It is also assumed in this model that the enolization of RFP^k to RFP is irreversible: in practice, this step is reversible, but the rate of this

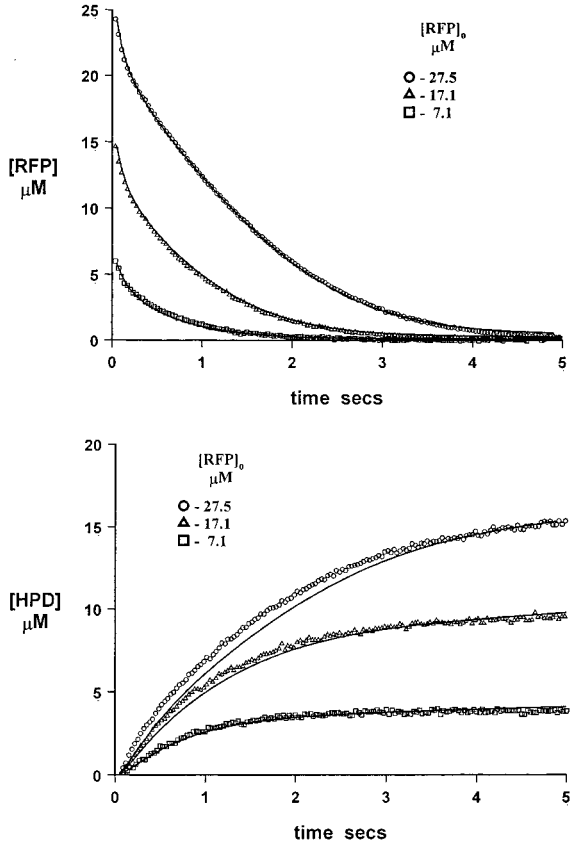

FIGURE 5: Pre-steady-state kinetic data measured for the MhpC-catalyzed reaction in 50 mM sodium citrate buffer, pH 4.0, modeled by branched kinetic model (see Scheme 3B).

step is so slow that it has only a very minor impact on the MhpC kinetic simulations.

The branched kinetic model was fitted to the concentration vs time datasets, giving the fits shown in Figure 5. Good correlation is observed for substrate disappearance, and there is a notably improved fit for the initial (<100 ms) timepoints, which are highly significant for data analysis. The observed fit to the product concentration data is reasonable, although there is some discrepancy at high substrate concentration. We ascribe this to a certain amount of decay of the unstable dienol product HPD, which occurs on a time scale of minutes in solution, but which is accelerated by MhpC (Pollard et al., 1997). However, significantly, there is a much better agreement for the branched kinetic model between the predicted intermediate concentration data and the observed data, even after several turnovers (see Figure 6). Thus, the branched kinetic model gives a significantly better description of the overall kinetic mechanism than the linear kinetic model.

The deduced kinetic constants are shown in Table 5. Compared with the values derived from the linear kinetic model, the initial K_s value is considerably smaller (30 μM), although still significantly larger than K_M. The predicted rate of release of RFP^k is 1.5 s^{-1}, the same as the rate of enzymatic processing of E·RFP^k, thus the enzyme is predicted to release 50% of the intermediate keto tautomer. The value of K_M can be calculated using eq 5.

$$K_M = \frac{K_S k_4(k_{-2} + k_3 + k_5)}{k_4(k_2 + k_{-2} + k_3 + k_5) + k_2 k_3} \qquad (5)$$

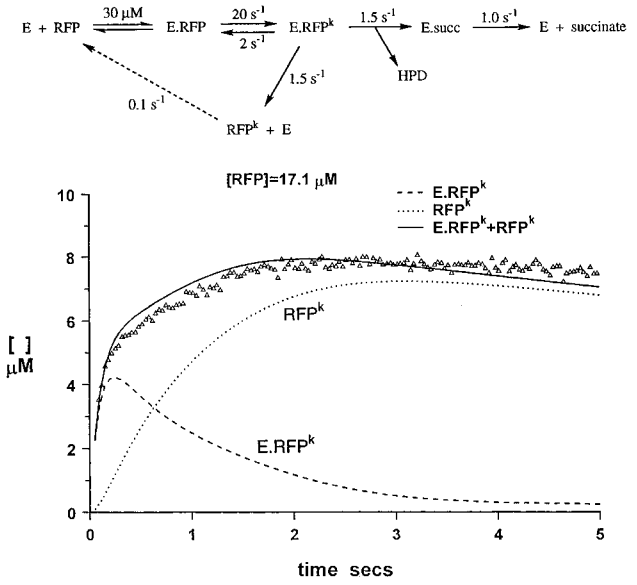

FIGURE 6: Concentration of free + enzyme-bound intermediate observed and calculated from the branched kinetic model for the [RFP] = 17.1 μM dataset. Inferred intermediate concentration (triangles) calculated by substraction of [RFP] and [HPD] from initial substrate concentration. Calculated values of [RFP^k] (dotted line), [E·RFP^k] (dashed line) and [RFP^k] + [E·RFP^k] are shown.

Table 5: Rate Constants Used in the Simulation of Stopped-Flow Experiments at pH 4.0 Using the Branched Kinetic Model[a]

step	symbol	value
E + RFP ↔ E·RFP	K_S	30 μM
E·RFP → E·RFP^k	k_2	20 s^{-1}
E·RFP^k → E·RFP	k_{-2}	2 s^{-1}
E·RFP^k → E·Succ + HPD	k_3	1.5 s^{-1}
E·Succ → E + Succ	k_4	1.0 s^{-1}
E·RFP^k → E + RFP^k	k_5	1.5 s^{-1}
RFP^k → RFP	k_6	0.1 s^{-1}

[a] Concentrations of RFP and MhpC were as in Table 3.

The calculated value for K_M from the values in Table 5 is 2.8 μM, which is in fair agreement with the experimental value of 7.0 μM. The steady-state rate equation has two values for k_{cat}, one for substrate disappearance (k_{cat}^{RFP}) and one for product (k_{cat}^{HPD}). The expressions for these are given in eqs 6 and 7.

$$k_{cat}^{RFP} = \frac{k_2 k_4(k_3 + k_5)}{k_4(k_2 + k_{-2} + k_3 + k_5) + k_2 k_3}$$

$$\frac{k_{cat}^{RFP}}{k_{cat}^{HPD}} = 1 + \frac{k_5}{k_3} \qquad (7)$$

The calculated value of k_{cat}^{RFP} is 1.1 s^{-1}, in agreement with the experimental value. It may be seen from Table 5 that $k_3 = k_5$ and that, therefore, k_{cat}^{HPD} is predicted to be half of k_{cat}^{RFP}. Previous work (Lam & Bugg, 1997) has shown that, under steady state at pH 8.0, the maximum observed rate of succinate production (which is equal to the rate of HPD production) is 15 s^{-1}, half that of RFP consumption (k_{cat} = 36 s^{-1}), consistent with these predictions. Thus, application of the branched kinetic model provides a better fit for both the pre-steady-state and steady-state kinetic behavior of hydrolase MhpC.

DISCUSSION

We have previously shown that the reaction catalyzed by hydrolase MhpC is stereospecific for insertion of the H-5_E proton, and that the enzyme catalyzes ^{2}H exchange into the H-5_Z position (Lam & Bugg, 1997). In order to seek evidence for the proposed keto-intermediate, we have analyzed the MhpC-catalyzed reaction using stopped-flow kinetics.

Each of the stopped-flow kinetic measurements is consistent with a kinetic mechanism involving a discrete intermediate in the catalytic cycle. We can conclude that this intermediate does not possess any significant new UV absorbances; therefore, its structure should be significantly less conjugated than either substrate or product. The structure of the proposed keto-intermediate would be consistent with these observations, and the inferred intermediate would be kinetically competent for the MhpC catalytic cycle.

Modeling of the stopped-flow data using a linear kinetic model gave a reasonable fit for substrate disappearance and product appearance (see Figure 3); however, the predicted concentration data for the keto-intermediate gave a poor fit to the inferred dataset (see Figure 4). Using a branched kinetic model in which the keto-intermediate is released at an appreciable rate from the active site, a much better fit to the dataset was obtained (see Figures 5 and 6). This provides confirmatory evidence for the release of the keto-intermediate, proposed in the previous paper in this issue to account for the MhpC-catalyzed ^{2}H exchange in the H-5_Z position.

Determination of individual rate constants for the second kinetic model reveals a K_s value of 30 μM for the dienol substrate, compared with a steady state K_M value of 7 μM (calculated value = 2.8 μM) under the same conditions. The disparity between these two values can be rationalized by the fast step ($k_2 = 20$ s^{-1}) following substrate binding, which strongly favors the keto-intermediate ($k_{-2} = 2$ s^{-1}). The keto-intermediate is then processed ($k_3 = 1.5$ s^{-1}) and released ($k_5 = 1.5$ s^{-1}) at equal rates. The final step is rate limiting ($k_4 = 1.0$ s^{-1}), but is not greatly slower than the previous step, consistent with the lack of burst of the product HPD. The rate of enolization of the released keto-intermediate to regenerate RFP appears to be relatively slow ($k_6 = 0.1$ s^{-1}), thus significant amounts of the keto-intermediate are predicted to accumulate during turnover.

This kinetic mechanism raises a number of mechanistic issues. Why is the enzyme active site so "leaky" with respect to the keto-intermediate, and why does the ketonization step favor the keto tautomer, when in solution the dienol tautomer is strongly favored? This apparent shift in equilibrium position could be due either to stabilization of the enzyme-bound keto-intermediate (E·RFP^k), or destabilization of the enzyme-bound substrate (E·RFP). The high K_s value and apparent "leakiness" suggest that the enzyme binds both the substrate dienol and the keto-intermediate relatively weakly, implying that substrate destabilization is most likely.

We suggest that the substrate may be bound in a strained, nonplanar conformation, as shown in Scheme 4. If the enzyme-bound substrate conformation positioned the C-6 carbonyl out of the plane of the dienol π system, then the inherent stability of the dienol would be removed, and the reactivity of the bound substrate would be changed. We have observed that the product dienol is much more reactive toward ketonization in aqueous solution (Pollard et al., 1997),

Scheme 4. Proposed Mechanistic Scheme for the MhpC-Catalyzed Reaction, Illustrating a Possible Nonplanar Conformation for the Enzyme-Bound Substrate[a]

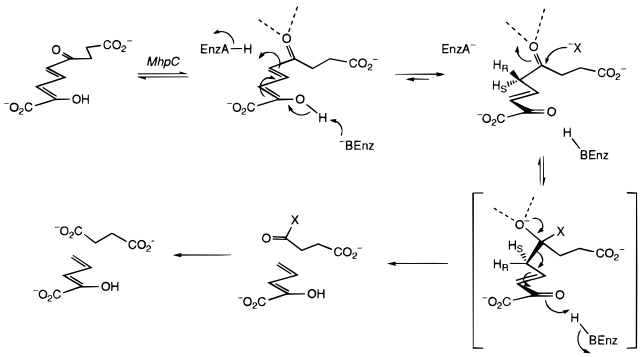

[a] X is either OH (from attack of water) or an active site nucleophile.

whereas the δ-keto dienol substrate is relatively stable. It is therefore reasonable to suppose that a twisted conformer in which the C-6 carbonyl group was out of planarity would be kinetically more reactive toward protonation and that such a ketonization step would be thermodynamically favorable at the enzyme active site. Other examples of enzymatic reactions which are thought to involve binding of substrate in a strained conformation include the binding of a flattened pyranose ring by lysozyme (Ford et al., 1974) and the binding of a twisted amide conformer by the peptidyl-proline *cis/trans* isomerases cyclophilin (Liu et al., 1990) and FKBP (Rosen et al., 1990; Albers et al., 1990). After ketonization, the intermediate contains an internal electron sink in the form of the α,β-unsaturated ketone, which facilitates C−C bond cleavage. The later steps might involve either base-catalyzed attack of water or attack of an active site nucleophile, generating in the latter case an acyl enzyme intermediate. Sequence similarity has been observed between the C−C hydrolases of bacterial *meta*-cleavage pathways and certain lipases and esterases (Horn et al., 1991), suggesting that the catalytic mechanism employs a serine catalytic triad (Diaz & Timmis, 1995; Ahmad et al., 1995). However, unlike the serine hydrolases, MhpC is still active at pH 4, and no burst of product release is observed. Hence, it remains to be determined whether an active site nucleophile is involved in this class of reactions.

In summary, the pre-steady-state kinetic analysis has provided evidence in support of a keto-intermediate, which appears to be formed via rapid ketonization of a strained enzyme−substrate complex. Given the apparent stability of the dienol substrate, it may be that destabilization upon substrate binding is a major contributing factor in the catalytic cycle of the C−C hydrolases.

ACKNOWLEDGMENT

The authors wish to thank Sarah Fleming for assistance in substrate preparation.

REFERENCES

Ahmad, D., Fraser, J., Sylvestre, M., Larose, A., Khan, A., Bergeron, J., Juteau, J. M., & Sondossi, M. (1995) *Gene 156*, 69−74.

Albers, M. W., Walsh, C. T., & Schreiber, S. L. (1990) *J. Org. Chem. 55*, 4984−4986.

Balls, A. K., & Wood, H. N. (1956) *J. Biol. Chem. 219*, 245−256.

Blakley, E. R., & Simpson, F. J. (1963) *Can. J. Microbiol. 10*, 175−185.

Cha, S. (1968) *J. Biol. Chem. 243*, 820−825.
Diaz, E., & Timmis, K. N. (1995) *J. Biol. Chem. 270*, 6403−6411.
Ford, L. O., Johnson, L. N., Machin, P. A., Phillips, D. C., & Tijan, R. (1974) *J. Mol. Biol. 88*, 349−371.
Horn, J. M., Harayama, S., & Timmis, K. N. (1991) *Mol. Microbiol. 5*, 2459−2474.
Hsiang, H. H., Sim, S. S., Mahuran, D. J., & Schmidt, D. E., Jr. (1972) *Biochemistry 11*, 2098−2102.
Kuliopulos, A., Mullen, G. P., Xue, L., & Mildvan, A. S. (1991) *Biochemistry 30*, 3169−3178.
Lam, W. W. Y., & Bugg, T. D. H. (1994) *J. Chem. Soc., Chem. Commun.* 1163−1164.
Lam, W. W. Y., & Bugg, T. D. H. (1997) *Biochemistry 36*, 12242−12256.
Liu, J., Albers, M. W., Chen, C. M., Schreiber, S. L., & Walsh, C. T. (1990) *Proc. Natl. Acad. Sci. U.S.A. 87*, 2304−2308.
Phillips, R. S., & Dua, R. K. (1991) *J. Am. Chem. Soc. 113*, 7385−7388.
Pollard, J. R., Henderson, I. M. J., & Bugg, T. D. H. (1997) *J. Chem. Soc., Chem. Commun.* (In press).
Press, W. H., Flannery, B. P., Teukolsky, S. A., & Vetterling, W. T. (1986) *Numerical Recipes*, Cambridge University Press, Cambridge, U.K.
Rosen, M. K., Standaert, R. F., Galat, A., Nakatsuka, M., & Schreiber, S. L. (1990) *Science 248*, 863−866.
Whitman, C. P., Aird, B. A., Gillespie, W. R., & Stolowich, N. J. (1991) *J. Am. Chem. Soc. 113*, 3154−3162.
Whitman, C. P., Hajipour, G., Watson, R. J., Johnson, W. H., Jr., Bembenek, M. E., & Stolowich, N. J. (1992) *J. Am. Chem. Soc. 114*, 10104−10110.

BI971116J